

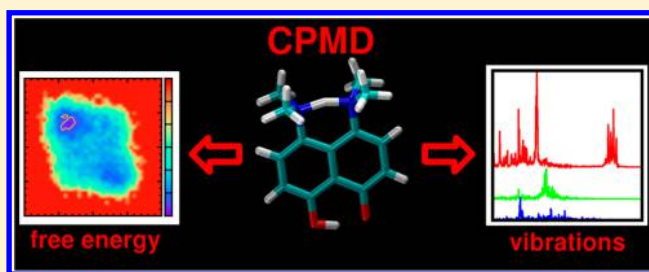
"Zwitterionic Proton Sponge" Hydrogen Bonding Investigations on the Basis of Car–Parrinello Molecular Dynamics

Aneta Jezierska* and Jarosław J. Panek

Faculty of Chemistry, University of Wrocław, ul. F. Joliot-Curie 14, 50-383 Wrocław, Poland

S Supporting Information

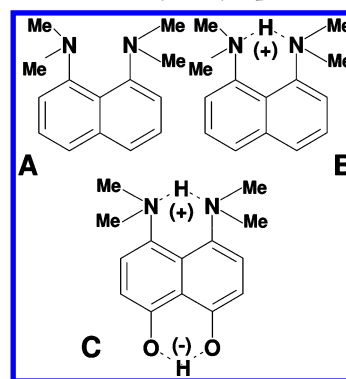
ABSTRACT: 1,8-Bis(dimethylamino)-4,5-dihydroxynaphthalene has been investigated on the basis of static DFT computations and Car–Parrinello molecular dynamics. The simulations were performed in the gas phase and in the solid state. The studied "zwitterionic proton sponge" possesses two, short intramolecular hydrogen bonds (O–H...O and N–H...N) classified as Low Barrier Hydrogen Bonds (LBHBs); therefore, the system studied is strongly anharmonic. In addition, the compound exists as a "zwitterion" in solution and in the solid state, thus the intramolecular hydrogen bonds belong to the class of charge-assisted interactions. The applied quantum-chemical methods enabled investigations of metric and spectroscopic parameters of the molecule. The time-evolution investigations of the H-bonding showed a strong delocalization of the bridge protons and their high mobility, reflected in the low barriers on the free energy surfaces. Frequent proton transfer phenomena were noticed. The power spectra of atomic velocity were computed to analyze the vibrational features associated with O–H and N–H stretching. A broad absorption was indicated for both hydrogen bridges. For the first time, Car–Parrinello molecular dynamics results are reported for the compound, and they indicate a broad, shallow but not barrierless, potential well for each of the bridge protons.



I. INTRODUCTION

In 1968 Alder et al. reported the first pK_a values for 1,8-diaminonaphthalenes.¹ They were interested in interactions between nonbonding electron pairs and discovered that 1,8-bis(dimethylamino)naphthalene (DMAN) undergoes an extremely easy protonation (see Chart 1A and B). Since that, the compound has become known in the literature as "proton sponge". The conformation of the compound is determined by interplay of several effects among which the steric inhibition of resonance, van der Waals repulsions, and dipole–dipole repulsions seem to be the most important. It exhibits a high flexibility, which is associated with the presence of the NMe_2 groups. The NMe_2 groups dynamics involve the rotation around $N-C_{ar}$, in-plane or out-of-plane movements where the distance between nitrogen atoms is modified, the change of the nitrogen's planarity which could be measured as a sum of valence angles at nitrogen atoms and nitrogen inversion which converts *in,in*-orientation of the nonbonded electron pairs (typical for most "proton sponges"), into less favorable *in,out* form.² DMAN has served as a parent compound for many new "proton sponges" e.g.^{2–11} and its protonated form (DMAN- H^+) has been as well an object of many studies^{12–18} related to the structure modification due to the intramolecular hydrogen bond formation. It has been found useful in crystal growth as agent deprotonating N–H acids as it was reported in many contributions e.g. ref 19. An interesting aspect is a property of the NHN^+ intramolecular hydrogen bond (IHB) and its spectroscopic implications. The hydrogen bond in DMAN and

Chart 1. Molecular Structures of 1,8-Bis(dimethylamino)naphthalene (DMAN) - A, Its Protonated Form - DMAN- H^+ - B, and 1,8-Bis(dimethylamino)-4,5-dihydroxynaphthalene - C^a



^aThe model of 1,8-bis(dimethylamino)-4,5-dihydroxynaphthalene was used for the static models and CPMD simulations in vacuo. Dotted lines indicate the presence of the O–H...O and N–H...N hydrogen bonds.

other "proton sponges" is characterized as short-strong-low barrier hydrogen bonding (LBHB). It has served as a model for proton transfer in enzymatic catalysis. It was found that in

Received: September 14, 2014

Published: May 12, 2015

solution the DMAN-H⁺ hydrogen bonding is symmetric in the NMR time-scale with the N–H proton centered between two nitrogen atoms. However, the system exhibits dynamics, which, in the view of low-temperature and time-resolved measurements in conjunction with some theoretical simulations, shows that the bridging proton in DMAN cation rapidly equilibrates near the symmetry plane (tunneling mechanism of hydrogen transfer).^{18,20} Therefore, the experimental and theoretical evidence provide us with an accurate description of the real situation which is expressed as equilibrium between two isoenergetic tautomers.

“Proton sponges” are discussed as well with respect to a borderline between low-barrier and barrier-free NHN⁺ hydrogen bonds. Such a situation was found by Degtyarev et al. in synthesized 1,8-bis(dimethylamino)-2,7-bis(trimethylsilyl)-naphthalene salt possessing a remarkably short [NHN]⁺ hydrogen bonding.¹⁵ The NHN⁺ bonding belongs to the charge-assisted hydrogen bond type. The specificity of the bonding in “proton sponges” was investigated by e.g. Sobczyk.¹⁶ It was reported that DMANH⁺ is characterized by a very low frequency for the NHN⁺ stretching vibrations, ca. 500 cm^{−1} and with an unusual ¹H/²H isotope effect opposite to that commonly observed, reaching values above 2. A double minimum with a very low barrier was found. The DMAN molecules have been studied computationally in the ground and excited states using semiempirical methods.²¹ On the basis of DMAN, many derivatives with various molecular features were synthesized and investigated, e.g. proton sponges with easily reversible basicity²² or potential receptor unit to develop sensitive fluorescent switches.²³ Thermochemical and structural properties of neutral DMAN, its protonated form, and naphthalene-based proton sponges were objects of study by Dávalos et al.²⁴

The motivation of the current work is associated with a better description and understanding of NHN⁺ and OHO[−] hydrogen bonding, present in 1,8-bis(dimethylamino)-4,5-dihydroxynaphthalene²⁵ (see Chart 1C). The compound exists as a zwitterion, which was confirmed experimentally by X-ray measurements. The unusual structure and excellent experimental results provided a good base for the current quantum-mechanical studies. Static and first-principle molecular dynamics models were developed to describe geometric, electronic structure parameters and spectroscopic signatures. The first models provided hydrogen bonding metric parameters description with proton potential functions describing the features of the IHB. Furthermore, the molecular topology of the “proton sponge” was examined on the basis of Atoms in Molecules (AIM).²⁶ The dynamical nature of the hydrogen bonding was explored on the basis of Car–Parrinello molecular dynamics (CPMD) in vacuo and in the crystalline phase.²⁷ The CPMD method has been applied successfully in our previous studies of compounds with LBHB e.g. refs 28–30.

Summarizing, the main aim of the study is detailed investigation of the proton dynamics with special attention paid to the proton transfer phenomena and spectroscopic signatures of the “proton sponge” obtained as power spectra from the CPMD runs.

II. COMPUTATIONAL METHODOLOGY

II.A. Static Models on the Basis of DFT and MP2. The energy minimization of 1,8-bis(dimethylamino)-4,5-dihydroxynaphthalene (see Chart 1C) was performed using the Gaussian09 vA02 and D.01 suite of programs.³¹ Density

functional theory (DFT)³² and Møller–Plesset second order perturbation theory (MP2)³³ were employed. The calculations were carried out using the hybrid B3LYP,^{34,35} PBE,³⁶ and wB97xD³⁷ functionals with various Pople’s triple- ζ split valence basis sets³⁸ and Dunning’s correlation consistent basis sets denoted as cc-pVTZ and aug-cc-pVTZ.³⁹ In addition, for B3LYP and PBE functionals empirical dispersion correction by Grimme⁴⁰ was used during the simulations. Harmonic frequencies were computed to confirm that the obtained structures correspond to the minima on the potential energy surface (PES). Subsequently, the reaction path of the bridge protons for O–H \cdots O and N–H \cdots N intramolecular hydrogen bonds were scanned for chosen levels of theory. The 0.1 Å increment for the O–H and N–H distances was applied. Either OHO or NHN valence angle was fixed, while the remaining part of the studied structure was left without any constraints. As a result, two series of distorted structures were obtained, and their energies were further used to construct the proton potential energy profiles.

The topology of 1,8-bis(dimethylamino)-4,5-dihydroxynaphthalene in equilibrium was investigated using the Atoms in Molecules (AIM) theory.²⁶ Special attention was devoted to the intramolecular hydrogen bonding. Electron density and its Laplacian were calculated at bond critical points (BCPs) providing a quantitative description of the hydrogen bonding.⁴¹ The AIM analysis was performed using the AIMPAC package,⁴² while the wave function for the computations was prepared within a framework of the Gaussian 09 vA2 and D.01 suite of programs.³¹

II.B. Car–Parrinello Molecular Dynamics in Vacuo and in the Crystalline Phase. Car–Parrinello molecular dynamics (CPMD)²⁷ was applied to develop time-evolution models for 1,8-bis(dimethylamino)-4,5-dihydroxynaphthalene (see Chart 1C). The simulations were carried out in vacuo and in the crystalline phase. The gas phase model used for CPMD runs is presented in Chart 1C, while the one for the solid-state simulations is presented in Figure S1. The energy minimization was performed for the studied compound in both phases with the initial Hessian matrix proposed by Schlegel.⁴³ The Perdew, Burke, Ernzerhof (PBE) functional³⁶ and Troullier–Martins pseudopotentials⁴⁴ were used in the study for both phases. The plane-wave computational setup was chosen after performing a series of tests described below. The kinetic energy cutoff values (range 70 Ry–120 Ry) were tested for the gas phase and solid-state models. The geometry minimization in the solid state was performed with Γ -point approximation (i.e., using only Bloch eigenfunctions with zero reciprocal vector k to represent the periodic states in the crystal)⁴⁵ and two sets of k -points mesh ($2 \times 2 \times 2$ and $3 \times 3 \times 3$).⁴⁶ On the basis of the test results (listed in the Supporting Information), the following setup for Car–Parrinello molecular dynamics was applied in the subsequent gas phase and solid-state computations. The kinetic energy cutoff for the plane-wave basis set was 100 Ry. The fictitious electron mass parameter was equal to 400 au. The time step was set to 3 au. The simulations were performed at room temperature ($T = 297$ K) and to control the assigned condition a Nosé–Hoover thermostat chain was applied.^{47–49} The computations were performed without and with dispersion correction according to Grimme.⁴⁰

The gas phase model (Chart 1C) was placed to a cubic cell with $a = 16$ Å, and the scheme of Hockney⁵⁰ was applied to remove interactions with periodic images of the cell. The translational and rotational movements were subtracted as well

Table 1. Electron Density and Its Laplacian Evaluated at Bond Critical Points (BCPs) of the Hydrogen Bridges in 1,8-Bis(dimethylamino)-4,5-dihydroxynaphthalene Computed at Various Levels of Theory ($\rho(e^*a_0^{-3})$ – Electron Density; $\nabla^2(\rho)(e^*a_0^{-5})$ – Laplacian of the Electron Density)

level of theory	AIM properties	O–H	H...O	N–H	H...N
B3LYP/6-311G(d,p)	$\rho(e^*a_0^{-3})$	0.29474	0.08161	0.27812	0.07768
	$\nabla^2(\rho)(e^*a_0^{-5})$	–1.85376	0.15604	–1.22855	0.08359
B3LYP/6-311+G(d,p)	$\rho(e^*a_0^{-3})$	0.29479	0.08001	0.27826	0.07774
	$\nabla^2(\rho)(e^*a_0^{-5})$	–1.87465	0.15406	–1.23239	0.08253
B3LYP/cc-pVTZ	$\rho(e^*a_0^{-3})$	0.29723	0.08554	0.28848	0.07836
	$\nabla^2(\rho)(e^*a_0^{-5})$	–1.99689	0.09263	–1.43222	0.04076
PBE/6-311G(d,p)	$\rho(e^*a_0^{-3})$	0.25159	0.10927	0.23661	0.10086
	$\nabla^2(\rho)(e^*a_0^{-5})$	–1.17049	0.10778	–0.77697	0.03307
PBE/6-311+G(d,p)	$\rho(e^*a_0^{-3})$	0.25205	0.10753	0.23697	0.10085
	$\nabla^2(\rho)(e^*a_0^{-5})$	–1.20022	0.10818	–0.78271	0.03188
MP2/6-311G(d,p)	$\rho(e^*a_0^{-3})$	0.29007	0.08513	0.25965	0.09187
	$\nabla^2(\rho)(e^*a_0^{-5})$	–1.84811	0.15773	–1.11983	0.06566
MP2/6-311+G(d,p)	$\rho(e^*a_0^{-3})$	0.28732	0.08452	0.25820	0.09313
	$\nabla^2(\rho)(e^*a_0^{-5})$	–1.83411	0.15399	–1.10579	0.06264

during the computations. The crystalline phase model was built on the basis of experimental X-ray data.²⁵ The experimental unit cell with $a = 9.325$ Å, $b = 10.648$ Å, $c = 13.773$ Å, $\beta = 106.95^\circ$ and with $Z = 4$ was used. The solid-state simulations were performed with periodic boundary conditions (PBCs) and with real-space electrostatic summations for the eight nearest neighbors in each direction (TESR = 8).

The CPMD simulations with the setup described above were performed without Grimme's dispersion correction (standard CPMD with 28 ps trajectory length for the gas phase and the solid state) and with the dispersion correction (28 ps trajectory for the gas phase and 14 ps for the solid state). The initial part of the MD run was taken as the equilibration, and the first 5000 steps were not considered for further analyses. The collected four sets of trajectories were used to analyze metric properties and free energy profiles of the studied compound in vacuo and in the crystalline phase. Further, additional CPMD runs using NVE ensemble, with no thermostating, were performed using final steps of the previous thermostated runs as restart points. The NVE runs (7.3 ps long in all the four cases) served to derive the spectroscopic properties of the system. The simulations were performed using the CPMD program v3.15.1.⁵¹ The data was analyzed with the VMD 1.8.6⁵² and Gnuplot⁵³ programs, as well as with locally written tools.

III. RESULTS AND DISCUSSION

The main aim of the study is devoted to a detailed analysis of hydrogen bonding properties in the studied “proton sponge”. The molecular properties of the compound have been studied on the basis of various theoretical approaches. Computationally obtained metric parameters have been compared directly with experimental data available. In the case of spectroscopic properties, related compounds have been used to support computational findings.

III.A. Static Models. The energy minimization was performed employing various levels of theory as it is presented in Tables S1, S2, and S3. A detailed discussion concerning the reproduction of experimental metric parameters and the performance of the applied theoretical approaches is given in the Supporting Information.

The proton potential energy was calculated at the DFT level of theory for B3LYP and PBE functionals with triple- ζ split-valence basis sets as it is presented in Figure S2. The flatness of

the obtained potential energy curves for both hydrogen bonds suggests highly anharmonic dynamics of both protons. As it is shown in the figure the energy barriers are low; therefore, a spontaneous proton transfer phenomenon is possible for both bridges. The shape of the obtained proton potential profiles has been very promising as a predictive source of information concerning the proton behavior and anharmonicity in the CPMD simulations. Ozeryanskii et al.⁵⁴ published experimental and quantum-chemical results for the studied molecule and some relative compounds. They discussed the tautomeric forms and proton equilibria in the studied set of compounds. They confirmed that 1,8-bis(dimethylamino)-4,5-dihydroxynaphthalene exists as a zwitterionic structure in solution and in the solid state. Semenov et al.¹¹ also reported on results for the “proton sponge” on the basis of DFT theory at the PBE0/cc-pV(D,T)Z levels. They investigated structural parameters, relative energies, and dipole moments of the prototropic tautomers. They found that according to their computations, the compound can exist in the gas phase as low-polar molecules with one asymmetric intramolecular hydrogen bond. However, in a polarizable medium a pair of zwitterionic tautomers dominate of similar energy with two asymmetric O–H...O and N–H...N hydrogen bonds. Their findings are in agreement with the data reported in ref 54.

Following, the structure investigations, the topology of the molecule was studied using the AIM theory. The electron density and its Laplacian were calculated at bond critical points (BCPs) related to the presence of the O–H...O and N–H...N intramolecular hydrogen bonds. The data for selected levels of theory is presented in Table 1. The obtained AIM results were further examined on the basis of Popelier's criteria⁴¹ for the hydrogen bonding. The first Popelier's criterion was met finding the presence of atomic interaction paths with respective critical points. Further criteria require that the critical points fulfill the following conditions: the electron density at the BCP at the hydrogen bond is in the range of 0.002–0.034 au (second Popelier's criterion), while its Laplacian is between 0.024 and 0.139 au (third Popelier's criterion). The application of the AIM theory confirmed the presence of the double hydrogen bonds in the studied “proton sponge”, placing them, additionally, at the extremely strong side of the scale (large electron density and its Laplacian at the HB BCPs).

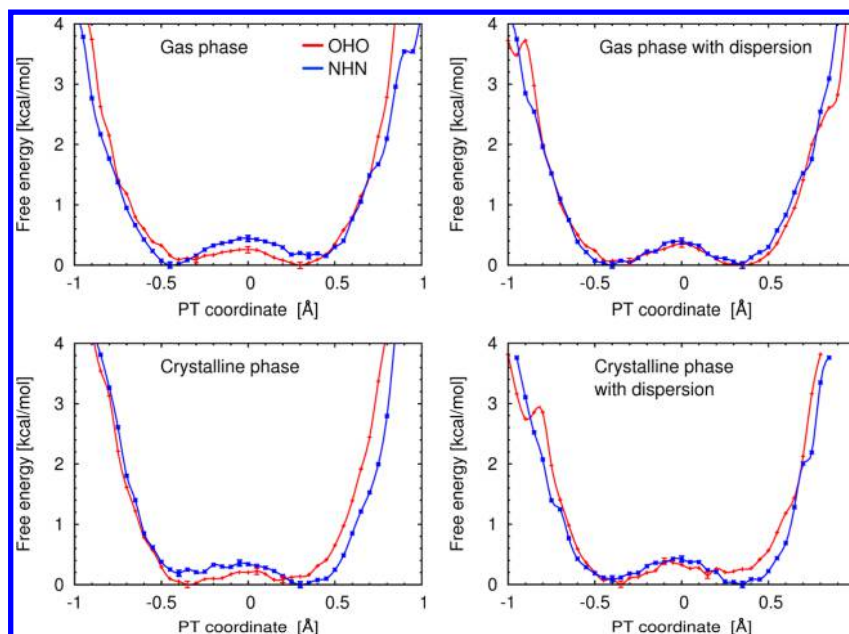


Figure 1. Free energy profiles for proton motion in the O–H···O (red) and N–H···N (blue) bridges of the studied compound. The proton transfer (PT) coordinate is defined as $r(A-H)-r(D-H)$, where D is the donor atom, A is the acceptor atom (this labeling is arbitrary because of the very large extent of proton sharing). Results of the FPMD runs. Error bars at minima and transition states represent statistical sampling of the free energy errors and are quite small; errors related to the DFT approach are expected to be much larger – see text for details.

III.B. Car–Parrinello Molecular Dynamics in the Gas Phase. Following previous gas phase findings for 1,8-bis(dimethylamino)-4,5-dihydroxynaphthalene on the basis of static models, Car–Parrinello molecular dynamics was applied to investigate time-evolution of metric and spectroscopic parameters. Let us start the discussion from the CPMD analysis of the O–H···O and N–H···H intramolecular hydrogen bonds. The time-evolution of interatomic distances of atoms involved in the intramolecular hydrogen bond formation is shown in Figure S3. Frequent proton transfer phenomena are observed for both hydrogen bonds. Concerning the O–H···O hydrogen bond, more frequent proton jumps are observed when the CPMD simulations have been performed without the dispersion correction. In the case of the N–H and H···N bonding a similar frequency of the proton transfer has been noticed. The analysis of the hydrogen bonding showed that in both analyzed bridges the proton is very labile and strongly delocalized. This is best visualized in the free energy surfaces for the proton motion in the bridges. The proton transfer (PT) coordinate, defined as the difference between the acceptor-proton and donor-proton distances, was selected as the basic coordinate, frequently used in the studies of PT, e.g. in liquid water.^{55–57} The data is presented in Figure 1 (one-dimensional representation along the PT coordinate) and Figure 2 (a two-dimensional surface with the PT coordinate and the donor–acceptor distance, i.e. bridge length, as the independent variables). The upper part of Figure 1 shows that the protons in both bridges move in a potential with a very small barrier, ca. 0.3 kcal/mol for the OHO and 0.45 kcal/mol for the NHN bridge. The barrier is located at 0 Å, corresponding to the proton equally shared between the donor and acceptor. The inclusion of the Grimme dispersion corrections makes the barriers almost equal (0.45 kcal/mol). Figure 2 (the upper part) shows this fact even more clearly. The inclusion of dispersion corrections results in a more visible separation of the two potential wells for the OHO bridge, while the NHN is not

affected. The obtained results are in agreement with previous gas phase models showing a strong delocalization of the bridge proton and confirm that the investigated hydrogen bond belongs to the class of LBHB. Further, the two bridges present different values of the bridge length: the OHO case is shorter (cf. the left and right columns of Figure 2) by ca. 0.15 Å. The inclusion of weak interactions showed the elongation of the bonding of ca. 0.05 Å with respect to the bond length obtained according to the standard CPMD simulation. In an effort to investigate the role of various factors in modifying the barrier height and shape, both accuracy of the DFT approach and statistical error of the free energy estimation must be taken into account. The obtained results show that the statistical errors are negligible in comparison with the DFT accuracy—the statistical error bars included for the minima and top of the barrier in Figure 1 are on the order of 0.1 kcal/mol. On the other hand, a recent study reviewing the accuracy of the DFT approaches for the proton transfer reactions shows that the PBE functional reproduces PT processes with mean unsigned error of ca. 2.2 kcal/mol, and values for other gradient-corrected pure DFT functionals are similar.⁵⁸ Additional calculations (see Table S4 of the SI and associated discussion therein) show that for the PBE-D2 approach, a similar error (2.5 kcal/mol) can be expected. It must be remembered, however, that the Grimme's D2 correction is an empirical potential added to the DFT total energy of the system. Therefore, it acts not by changing the physics of the underlying DFT functional but by forcing the system to be placed in a slightly different position on the PES. In case of the studied molecule, with its aromatic system, a rather uniform behavior of the PBE functional over various proton positions can be expected, because the investigated processes do not involve change of covalent bond types etc. Summarizing, our results so far do not bring strong evidence that the dispersion plays significant role, and further statistical (correlational) analysis will be carried out below to support this statement.

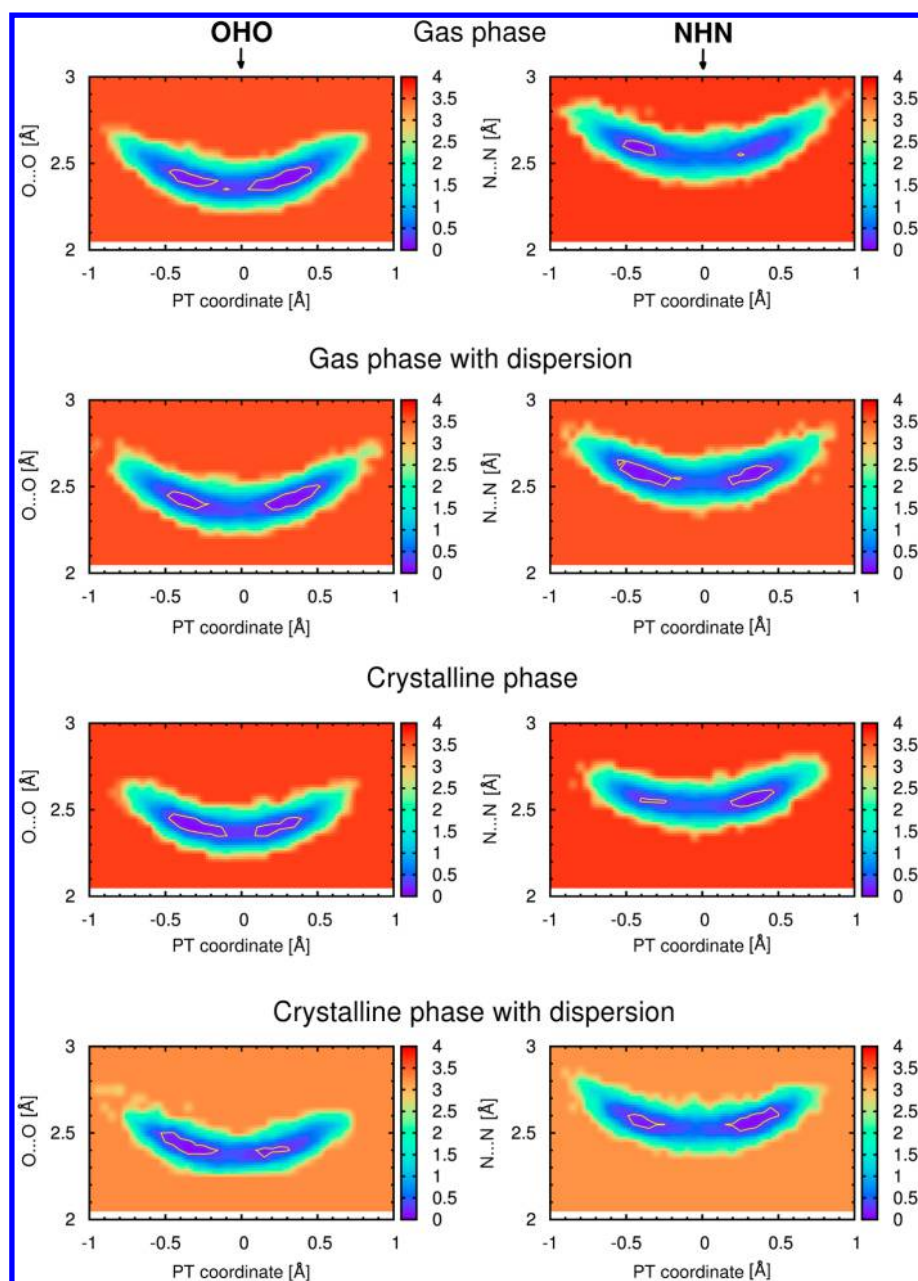


Figure 2. Two-dimensional free energy surfaces for proton motion in the O–H...O (left column) and N–H...N (right column) bridges of the studied compound. The color scale represents free energy values, in kcal/mol. The proton transfer (PT) coordinate on the horizontal axis is defined as $r(\text{A}–\text{H})–r(\text{D}–\text{H})$; the vertical axis represents the D...A distance, where D is the donor atom, and A is the acceptor atom. Yellow isoline at 0.25 kcal/mol indicates the minima. Results of the FPMD runs.

Next, a study of correlation between the bridges was carried out. Figure S4 presents a few selected fragments of the trajectory. It is shown that the bridge protons reside at a chosen site (donor or acceptor) for a time visibly larger than the time of the “jump” event, however without apparent correlation between bridges. Figure 3 reveals, however, that such a correlation exists. It shows the free energy surface using PT coordinates of both bridges as independent variables. Its upper part, related to the gas phase CPMD results, shows that, indeed, inclusion of dispersion heightens the barrier and makes “synchronous transit of the protons” less probable. Even more interestingly, the protons prefer *trans* arrangement with respect to the center of the molecule (see Chart 2). It is in agreement with chemical intuition and the properties of the

bonding. The chemical composition of the system – a presence of two fused rings with aromatic features, quasi-rings formation as a result of the intramolecular hydrogen bonding and CH_3 substituents in the amino moiety – makes the discussion of the hydrogen bridges complicated, because of possible inductive and steric effects. However, Chart 2 offers a qualitative explanation: the *trans* arrangement of the protons maximizes attraction between the centers of formal charges of the opposite sign. The attraction can be transferred not only by space but also via the aromatic skeleton. This makes the studied compound an ideal case for modifications (e.g., introduction of asymmetric substituents to break the symmetry of bridge potential wells). Especially, the presence of the inductive effects has always an impact on the hydrogen bonding.⁵⁹ However, the

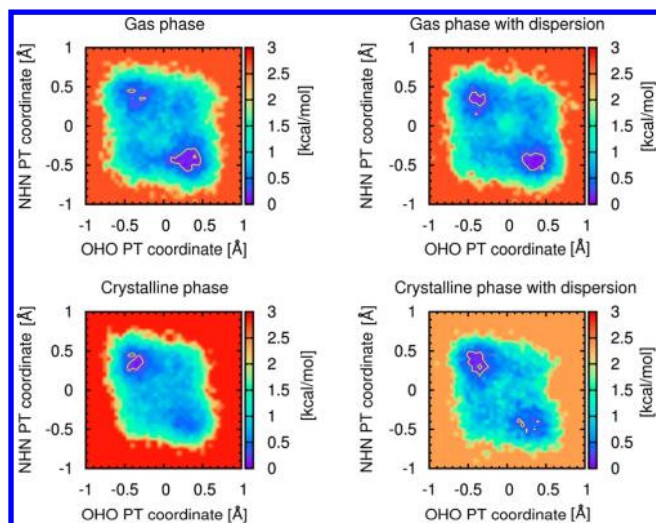
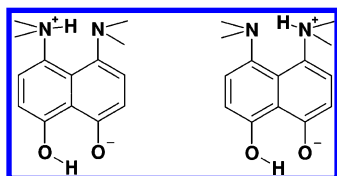


Figure 3. Two-dimensional free energy surfaces showing correlation of proton motion in the O–H...O and N–H...N bridges of the studied structure. The color scale represents free energy values, in kcal/mol. The proton transfer (PT) coordinates are defined as $r(\text{A}-\text{H})-r(\text{D}-\text{H})$, where D is the donor atom, and A is the acceptor atom. Yellow isoline at 0.25 kcal/mol indicates the minima. Results of the FPMD runs.

Chart 2. Qualitative Explanation of the Phenomenon Seen in Figure 3^a



^aThe bridge protons prefer arrangement pictured on the right, not on the left, because it maximizes attraction between the centers of formal charges of the opposite sign.

correlations are not strong. In order to trace the correlations fully, the results for the solid state are included here in anticipation. The correlation coefficients between the two displacement variables are, respectively, for the different simulation regimes: $r = -0.344$ in the gas phase, -0.394 in the gas phase with Grimme dispersion included, -0.439 in the crystal, and finally -0.467 in the crystal with dispersion correction. This shows that, on the one hand, the protons move rather freely and the correlation of their movements is not perfect, but on the other hand – there is a systematic increase in the correlation coefficient when the dispersion correction is taken into account and – even stronger – when going from the isolated molecule to the solid state. The negative sign of the correlation coefficient is consistent with the explanation given above on the basis of Chart 2.

Hydrogen bonding, especially a strong, LBHB case found in the studied system, has strong impact on the spectroscopic signatures. Therefore, the spectroscopic features of the studied molecule will be discussed. Unfortunately, the data analysis will cover only the computational findings, and some conclusions will be drawn on the basis of relative compounds, because of lack of experimental IR spectra. The dynamics of both bridge protons is reflected in the power spectra of atomic velocity. The computed spectra for the gas phase CPMD simulation with Grimme corrections are presented in Figure 4, and Figures S6–

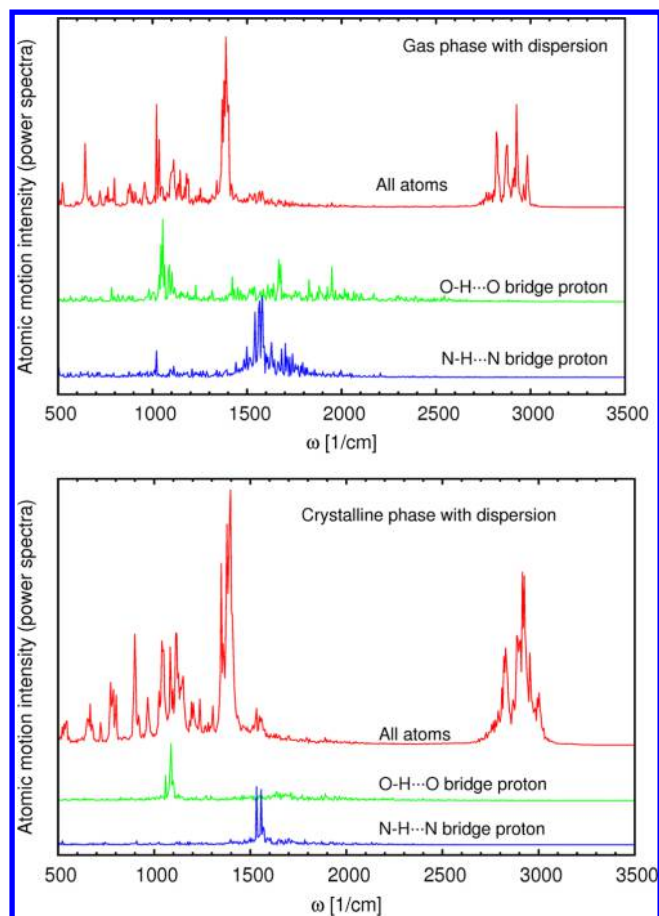


Figure 4. Fourier transforms of the atomic velocity autocorrelation function for the studied 1,8-bis(dimethylamino)-4,5-dihydroxynaphthalene. The results obtained from FPMD run (NVE ensemble) in the gas phase and in the crystalline phase with dispersion correction.

S12 present further details of this and other simulations (the additional graphical presentation of the spectroscopic signatures was prepared to provide comparison of various results, and it will not be discussed in detail, apart from a mention that the application of the thermostat chains introduces artifacts to the shape of the particular signals, although it affects the ranges covered by signals of the specified protons in the power spectra only to a small extent). The upper part of Figure 4 presents the total contribution of all atoms to the vibrational power spectrum together with the isolated bridge protons. The power spectra of “all atoms” show two well-separated regions: 500–1600 cm^{-1} and 2750–3000 cm^{-1} , the latter corresponding to the C–H stretching. It is difficult using the all-atom spectra to identify the O–H or N–H stretching positions; therefore, the bridge protons were plotted separately, and they are presented in the same figure. The broad absorption range of the O–H motions is located between 500 and 2200 cm^{-1} . A similar picture of a broad frequency range was found for the N–H motions, and the continuous absorption range was found between 500–2100 cm^{-1} . Concerning the O–H stretching, two main regions of higher motion intensity could be distinguished: 1000–1100 cm^{-1} and 1400–2200 cm^{-1} . The N–H motion has most intensity located in the 1400–1900 cm^{-1} region. As it is shown in the Figures S6–S12 the inclusion of dispersion effects did not change the computed vibrational modes of the studied molecule. The difference between the two types of bridges is visible in the vibrational signatures, even if

the stretching regions overlap. The extremely low wavenumber values correspond to a very strong LBHB, which is consistent with the NMR data for the studied compound in DMSO solution: the chemical shift is 18.10 ppm for the NHN^+ proton and 19.30 ppm for the OHO^- proton.²⁵ This is in agreement with metric parameters analysis from where a strong mobility of the bridge proton and its delocalization were predicted.

The obtained stretching modes are estimated to be red-shifted (ca. 100 cm^{-1}) by introduction of various effects: the DFT functional, pseudopotential, finite cutoff (basis set effect), and finally, the Car–Parrinello “drag effect” inherent to the Car–Parrinello scheme.⁶⁰ The “drag effect” is caused by finite fictitious mass of the orbital coefficients treated as dynamical parameters in the CPMD. This, in turn, couples the electronic and ionic degrees of freedom. The result is not only a red shift of the vibrational wavenumbers (which is mode-dependent)⁶⁰ but also, for example, the fact that diffusion coefficients in water calculated from the CPMD runs can be up to two times larger than those computed from the Born–Oppenheimer MD calculations.⁶¹ Moreover, CPMD can introduce errors in the forces acting on nuclei even if otherwise the simulation seems to be converged.⁶² The fictitious orbital mass used in the current study, 400 au, was found to yield ca. 150 cm^{-1} red shift for the HF molecule with respect to the experimentally derived harmonic frequency,⁶³ and – for the current system – the best estimator of this effect is the location of the C–H bands. They are well-established experimentally to be located at $2850\text{--}3000\text{ cm}^{-1}$ in alkanes and up to 3100 cm^{-1} in arenes; in the studied case (see Figure 4) the C–H signals are located between 2750 and 3000 cm^{-1} , which corresponds to a red shift of up to 100 cm^{-1} . This is also a tentative estimate of the red shift for other modes in the system.

III.C. Car–Parrinello Molecular Dynamics in the Crystalline Phase. The last part of the computations was devoted to the crystalline phase investigations on the basis of CPMD. CPMD in the solid state enables the reproduction of the environmental influence (e.g., electrostatic polarization by the neighboring molecules), because the computations are performed with periodic boundary conditions (PBCs). The time-evolution of interatomic distances in the investigated bridges is shown in Figure S3. Similarly to the gas phase, in the crystalline phase, for both hydrogen bridges, frequent proton transfer phenomena have been observed. Interestingly, the inclusion of the dispersion effects has changed the frequency of the proton transfer events in both bridges: the time between jumps (i.e., the residence time at a chosen donor or acceptor site) is longer than without the dispersion correction. Figure 1 (its lower part) shows the reason for this behavior: in similarity to the gas phase results, inclusion of the Grimme correction raises the barrier for the OHO bridge, making it almost identical to that found for the NHN bridge. Still, the barriers, located at 0 of the PT coordinate, are very low (less than 0.45 kcal/mol), allowing for frequent proton jumps between the two wells. For reasons discussed in Section III.B above, the influence of dispersion correction is only tentatively assigned. The lower part of Figure 2 contains 2D free energy surfaces with donor–acceptor distance as the second coordinate. The wells are separated by an increased barrier when the dispersion correction is included, and an apparent asymmetry of the wells, visible already in Figure 1, is also present. The origin of this asymmetry can be found in the environment effect of the crystal field, which does not match the symmetry of the molecule (for example, the nearest distances between an

oxygen atom of one molecule and nitrogen atom of its neighbor are 3.766 and 3.776 Å – for details, see Figure S5).²⁵ The loss of symmetry is small, but also the free energy profiles have small barriers and are easily modifiable. The correlation between the bridges (see the bottom part of Figure 3) is similar to that found in the gas phase, with preferred *trans* arrangement of the bridge protons (Chart 2). It is worth noting that, on the basis of Figure 1 and Figure S5, one can expect more pronounced symmetry breaking of the bridges in the solid state. This was already shown in Section III.B, where correlation coefficients for the variables used in Figure 3 were described. The effect of the crystal electrostatic field was much stronger than the effect of dispersion correction. The experimental data²⁵ fully correspond to the computational results with Grimme’s correction (Figure 1, bottom right panel), where the OHO bridge should exhibit large deviation from symmetry than the NHN moiety. However, the experiment based on an X-ray diffraction has inherently large uncertainty in determination of the proton position, and further investigation of this interesting case should involve temperature-dependent neutron diffraction measurements, in a manner similar to a study on the $\text{O}\cdots\text{H}\cdots\text{N}$ bond with thermally induced proton migration.⁶⁴ Concluding, it has been shown that the Grimme’s correction has a larger influence on the hydrogen bridge dynamics in the crystalline phase than in vacuo in the case of the studied “proton sponge”. The barriers are very small and allow for frequent PT events.

The power spectra of the atomic velocity for the crystalline phase are presented in Figure 4 (lower part) and Figures S6–S12. In Figure 4 the spectrum for “all atoms” shows two absorption regions: $500\text{--}1600\text{ cm}^{-1}$ (heavy atom stretchings, bendings, torsions) and $2750\text{--}3050\text{ cm}^{-1}$ (C–H stretching). The broad absorption regions of O–H and N–H are much less pronounced than in the gas phase and were found between $1000\text{--}2000\text{ cm}^{-1}$ and $1400\text{--}2000\text{ cm}^{-1}$, respectively. The O–H maxima of intensity occur at 1150 cm^{-1} , and there is a broad, barely pronounced maximum at ca. 1600 cm^{-1} . For the N–H motion, the maximum intensity is at 1550 cm^{-1} . The broad absorption indicates that the O–H and N–H stretchings are strongly coupled (in consistency with Figure 3) and correlate with the remaining modes of both bridges (this follows from Figure 2) and possibly also other intramolecular vibrations. The inclusion of the dispersion correction did not change the spectroscopic signatures of the studied system as it is shown in Figures S11 and S12. The broad absorption regions confirm a strong delocalization of the bridge proton in both hydrogen bonds. The environmental effects of the solid state do not change significantly the vibrational features; this is in contrast to some of our earlier CPMD results³⁰ but is easily explained by the zwitterionic nature of the isolated molecule. A strong charge-assisted strengthening of the HBs is already present in the gas phase. However, both static calculations and the details of the CPMD runs (Figures 1–3, S3, and S4) lead to the conclusion that the potential well is not absolutely barrierless (i.e., a single-well potential). Time evolution of the interatomic distances (Figures S3 and S4) show that the protons reside at a chosen site (donor or acceptor) for a time visibly larger than the time of the “jump” event, which is consistent with the presence of a small barrier (Figures 1–3). However, the spectroscopic picture of the compound within the spectroscopic methods with time scale longer than several picoseconds (e.g., NMR) could be symmetric (the protons located, apparently, “in the middle”). The computational findings for

NHN⁺ are in agreement with IR measurements reported for relative compounds by Sobczyk.¹⁶ DMANH⁺ is characterized by very low frequency $\nu(\text{NHN})^+$ stretching vibrations at ca. 500 cm⁻¹, which are consistent with the gas phase and solid-state CPMD results. More detailed conclusions on the accuracy of the predicted spectrum are prevented by the lack of IR data for the (OHO)⁻ bridges in analogous proton sponges. The strong delocalization of the protons suggests that the NHN and OHO stretching modes will heavily overlap (see Figure 4) making the experimental investigation difficult. However, the shape of the free energy profiles calls for extended temperature-dependent experimental studies of vibrational and NMR properties of 1,8-bis(dimethylamino)-4,5-dihydroxynaphthalene. It is to be expected that at low temperatures, when the thermal energy becomes smaller than the barrier height, an interesting interplay will take place between trapping the protons in one of the wells and the nuclear quantum effects (NQE). The studied system, either in gas phase or in the crystal, exhibits very low barriers for the proton motion in the bridge (see Figures 1–3), which are comparable to, or even smaller than, the thermal energy accessible to the oscillators ($k_B T$ at 300 K is ca. 0.6 kcal/mol). In such a case, the influence of the NQE on the properties we are mostly interested in, that is spectroscopic signatures, which do not depend strongly on rare events (located high on the free energy surface, separated by a high barrier), is relatively small.⁵⁷ The role of NQE in such a case is mostly concerned with larger delocalization of the proton particles, provided by the quantum vibrational zero-point motion, and not by the tunneling, because after inclusion of the NQE, the barrier would lie below the lowest vibrational eigenvalue, whereas in the classical regime the PT events are already quite frequent.⁵⁵ This discussion is meaningful for spectroscopic properties (e.g., red shifts of the proton vibrational signatures), but the inclusion of NQE will have strong impact on the form of the free energy surface itself. In case of small barriers encountered here, the quantization of nuclear motions will result in barrierless energy surfaces. This will have impact on the choice of methods of studying the NQE in 1,8-bis(dimethylamino)-4,5-dihydroxynaphthalene (see the end of the Conclusions).

IV. CONCLUSIONS AND PERSPECTIVES

Herein, 1,8-bis(dimethylamino)-4,5-dihydroxynaphthalene was investigated, which exists as a zwitterion in solution and in the solid state. The compound possesses two intramolecular hydrogen bonds responsible for the structure stabilization and quasi-rings formation. X-ray crystallographic results were compared with computed data derived from static and ab initio molecular dynamics methods. Metric and spectroscopic features of the studied “proton sponge” were investigated. It was found that applied levels of theory are able to reproduce correctly the interatomic distances of atoms involved in the intramolecular hydrogen bonds. The DFT level of theory was applied to obtain proton potential profiles in both bridges. It was found that the energy barriers are very low, and spontaneous proton transfer phenomena occurs. The promising results based on the static simulations encouraged further CPMD simulations with and without Grimme’s dispersion corrections. The simulations were performed in vacuo and in the solid state. The time-evolution results and free energy surfaces derived therefrom showed high mobility of both bridge protons as well as their strong delocalization. The dispersion correction seems to have a stronger influence in the crystalline phase than in the gas phase. An interesting correlation of the

proton motions was found on the basis of the 2D free energy surfaces. The power spectra of atomic velocity provided spectroscopic signatures for the investigated molecules, and they are in agreement with metric findings concerning the protons delocalization and strengths of the hydrogen bonds. The results indicate unusual flatness (but with some barrier still present) of both potential wells in a single structure connected by aromatic subsystem. This provides ideal case for modifications, for example introduction of asymmetric substituents to break the symmetry of bridge potential wells. The investigated compound is an interesting object for further studies, which will include a quantum treatment of the atomic nuclei. Further studies are in progress, and we focus on free energy profiles determination on the basis of metadynamics method to have greater control of the phase space sampling.⁶⁵ Path integral molecular dynamics (PIMD) will be employed to show the quantization of atomic nuclei influence on the metric parameters with special attention paid to the double hydrogen bonding features, including the shape of the associated free energy surface. The quantization of the O–H and N–H vibrational properties will be done with the use of an “envelope method”, based on an *a posteriori* solution of a vibrational Schrödinger equation for a set of snapshots from the CPMD trajectory.^{66,67}

■ ASSOCIATED CONTENT

Supporting Information

Graphical representation of the solid-state unit cell, tabulated data for optimization of the structure at different levels of theory, extended discussion of the structural parameters from the static calculations, results of the plane-wave setup validation, details of the CPMD trajectories, additional representations of the vibrational signatures, and discussion of the accuracy of the PBE-D2 model. The Supporting Information is available free of charge on the ACS Publications website at DOI: 10.1021/ci500560g.

■ AUTHOR INFORMATION

Corresponding Author

*Phone: 48 71 3757 224. Fax: 48 71 3282 348. E-mail: aneta.jezierska@chem.uni.wroc.pl.

Notes

The authors declare no competing financial interest.

■ ACKNOWLEDGMENTS

The authors would like to express their thanks to the Wrocław Centre for Networking and Supercomputing (WCSS), Academic Computer Center CYFRONET-KRAKOW (Grant: KBN/SGI/UWrocl/078/2001,) and Centre at the ICM, University of Warsaw (grant no. G52-7) for generous grants of the computing time and use of file storage facilities. The authors would also like to thank the National Science Centre (Poland) for supporting this study under the grant no. UMO-2011/03/B/ST4/00699.

■ REFERENCES

- (1) Alder, R. W.; Bowman, P. S.; Steele, R. S.; Winterman, D. R. The Remarkable Basicity of 1,8-Bis(Dimethylamino)Naphthalene. *Chem. Commun.* **1968**, 452, 723–724.
- (2) Boiko, L. Z.; Sorokin, V. I.; Filatova, E. A.; Starikova, Z. A.; Ozeryanskii, V. A.; Pozharskii, A. F. Three Examples of Naphthalene Proton Sponges with Extreme or Unusual Structural Parameters.

General View on Factors Influencing Proton Sponge Geometry. *J. Mol. Struct.* **2011**, *1005*, 12–16.

(3) Cox, C.; Wack, H.; Lektka, T. Strong Hydrogen Bonding to the Amide Nitrogen Atom in an “Amide Proton Sponge”: Consequences for Structure and Reactivity. *Angew. Chem., Int. Ed.* **1999**, *38*, 798–800.

(4) Malarski, Z.; Lis, T.; Olejnik, Z.; Grech, E.; Nowicka-Scheibe, J.; Majerz, I.; Sobczyk, L. Proton Sponge as a Deprotonating Agent in Crystal Engineering. Structure and IR Spectra of Double-Deprotonated 1,5-bis(p-toluenesulphonamido)-2,4,6,8-tetranitronaphthalene in the DMAN Adduct. *J. Mol. Struct.* **2000**, *552*, 249–256.

(5) Bucher, G. DFT Calculations on a New Class of C3-Symmetric Organic Bases: Highly Basic Proton Sponges and Ligands for Very Small Metal Cations. *Angew. Chem., Int. Ed.* **2003**, *42*, 4039–4042.

(6) Szemik-Hojniak, A.; Zwier, J. M.; Buma, W. J.; Bursi, R.; van der Waals, J. H. Two Ground State Conformers of the Proton Sponge 1,8-bis(dimethylamino)naphthalene Revealed by Fluorescence Spectroscopy and Ab Initio Calculations. *J. Am. Chem. Soc.* **1998**, *120*, 4840–4844.

(7) Ozeryanskii, V. A.; Pozharskii, A. F.; Koroleva, M. G.; Shevchuk, D. A.; Kazheva, O. N.; Chekhlov, A. N.; Shilov, G. V.; Dyachenko, O. A. N,N,N'-Trialkyl-1,8-diaminonaphthalenes: Convenient Method of Preparation from Protonated Proton Sponges and the First X-Ray Information. *Tetrahedron* **2005**, *61*, 4221–4232.

(8) Raab, V.; Gauchenova, E.; Merkoulov, A.; Harms, K.; Sundermeyer, J.; Kovačević, B.; Maksić, Z. B. 1,8-Bis-(hexamethyltriaminophosphazenylnaphthalene, HMPN: a Superbasic Bisphosphazene “Proton Sponge”. *J. Am. Chem. Soc.* **2005**, *127*, 15738–15743.

(9) Singh, A.; Ganguly, B. Rational Design and First-Principles Studies Toward the Remote Substituent Effects on a Novel Tetracyclic Proton Sponge. *J. Phys. Chem. A* **2007**, *111*, 6468–6471.

(10) Mazaleyrat, J.-P.; Wright, K. Binaphthyl Substituted 1,8 bis(dimethylamino)naphthalenes, the First Chiral, Atropisomeric, Proton Sponges. *Tetrahedron Lett.* **2008**, *49*, 4537–4541.

(11) Semenov, S. G.; Makarova, M. V. Tautomers of 4,5-dihydroxy-1,8-bis(dimethylamino)naphthalene and Related Boron Compounds: A Quantum-Chemical Study. *Russ. J. Gen. Chem.* **2012**, *82*, 899–905.

(12) Mallinson, P. R.; Woźniak, K.; Smith, G. T.; McCormack, K. L. A Charge Density Analysis of Cationic and Anionic Hydrogen Bonds in a “Proton Sponge” Complex. *J. Am. Chem. Soc.* **1997**, *119*, 11502–11509.

(13) Eitner, K.; Schroeder, G.; Rybachenko, V. I.; Brzezinski, B. NHN+ Intramolecular Hydrogen Bonds: Heat of Formation and Parameters of Some Proton Sponges. *J. Mol. Struct.* **2000**, *525*, 247–251.

(14) Ozeryanskii, V. A.; Shevchuk, D. A.; Pozharskii, A. F.; Kazheva, O. N.; Chekhlov, A. N.; Dyachenko, O. A. Protonation of Naphthalene Proton Sponges Containing Higher N-Alkyl Groups. Structural Consequences on Proton Accepting Properties and Intramolecular Hydrogen Bonding. *J. Mol. Struct.* **2008**, *892*, 63–67.

(15) Degtyarev, A. V.; Ryabtsova, O. V.; Pozharskii, A. F.; Ozeryanskii, V. A.; Starikova, Z. A.; Sobczyk, L.; Filarowski, A. 2,7-Disubstituted Proton Sponges as Borderline Systems for Investigating Barrier-Free Intramolecular Hydrogen Bonds. Protonated 2,7-bis(trimethylsilyl)- and 2,7-di(hydroxymethyl)-1,8-bis(dimethylamino)-naphthalenes. *Tetrahedron* **2008**, *64*, 6209–6214.

(16) Sobczyk, L. The Specificity of the [NHN]+ Hydrogen Bonds in Protonated Naphthalene Proton Sponges. *J. Mol. Struct.* **2010**, *972*, 59–63.

(17) Pozharskii, A. F.; Ozeryanskii, V. A. Proton Sponges and Hydrogen Transfer Phenomena. *Mendeleev Commun.* **2012**, *22*, 117–124.

(18) Ozeryanskii, V. A.; Pozharskii, A. F. Simple and Hydrolytically Stable Proton Sponge Based Organic Cation Displaying Hydrogen Bonding and a Number of Related Phenomena. *Tetrahedron* **2013**, *69*, 2107–2112.

(19) Głowiak, T.; Malarski, Z.; Sobczyk, L.; Grech, E. New Example of a Symmetric NHN Hydrogen Bond in Protonated 1,8-bis-

(dimethylamino)naphthalene (DMAN). *J. Mol. Struct.* **1992**, *270*, 441–447.

(20) Bernatowicz, P.; Kowalewski, J.; Sandström, D. NMR Relaxation Study of the Protonated Form of 1,8-bis(dimethylamino)naphthalene in Isotropic Solution: Anisotropic Motion Outside of Extreme Narrowing and Ultrafast Proton Transfer. *J. Phys. Chem. A* **2005**, *109*, 57–63.

(21) Szemik-Hojniak, A.; Deperasinska, I.; Allonas, X.; Jacques, P. Inversion of States in Two Conformers of 1,8-bis(dimethylamino)naphthalene—the Proton Sponge. *J. Mol. Struct.* **2000**, *526*, 219–225.

(22) Ozeryanskii, V. A.; Pozharskii, A. F.; Milgizina, G. R.; Howard, S. T. Synthesis and Properties of 5,6-Bis(dimethylamino)-acenaphthylene: The First Proton Sponge with Easily-Modified Basicity. *J. Org. Chem.* **2000**, *65*, 7707–7709.

(23) Xiao, Y.; Meiyang, Fu, M.; Qian, X.; Cui, J. A Proton Sponge-Based Fluorescent Switch. *Tetrahedron Lett.* **2005**, *46*, 6289–6292.

(24) Dávalos, J. Z.; Lago, A. F.; Costa, J. C. S.; Santos, L. M. N. B. F.; González, J. Thermochemical and Structural Properties of DMAN-“Proton Sponges”. *J. Chem. Thermodyn.* **2012**, *54*, 346–351.

(25) Staab, H. A.; Krieger, C.; Hieber, G.; Oberdorf, K. 1,8-Bis(dimethylamino)-4,5-dihydroxynaphthalene, a Neutral, Intramolecularly Protonated “Proton Sponge” with Zwitterionic Structure. *Angew. Chem., Int. Ed. Engl.* **1997**, *36*, 1884–1886.

(26) Bader, R. F. W. Atoms in Molecules. *A Quantum Theory*; Clarendon: Oxford, 1990.

(27) Car, R.; Parrinello, M. Unified Approach for Molecular Dynamics and Density-Functional Theory. *Phys. Rev. Lett.* **1985**, *55*, 2471–2474.

(28) Jezierska, A.; Panek, J. J.; Mazzarello, R. Structural and Electronic Structure Differences Due to the O–H•••O and O–H•••S Bond Formation in Selected Benzamide Derivatives: a First-Principles Molecular Dynamics Study. *Theor. Chem. Acc.* **2009**, *124*, 319–330.

(29) Jezierska, A.; Panek, J. J.; Koll, A. Spectroscopic Properties of a Strongly Anharmonic Mannich Base N-oxide. *ChemPhysChem* **2008**, *9*, 839–846.

(30) Jezierska-Mazzarello, A.; Panek, J. J.; Vuilleumier, R.; Koll, A.; Ciccotti, G. Direct Observation of the Substitution Effects on the Hydrogen Bridge Dynamics in Selected Schiff Bases—A Comparative Molecular Dynamics Study. *J. Chem. Phys.* **2011**, *134*, 034308.

(31) Frisch, M. J.; Trucks, G. W.; Schlegel, H. B.; Scuseria, G. E.; Robb, M. A.; Cheeseman, J. R.; Scalmani, G.; Barone, V.; Mennucci, B.; Petersson, G. A.; Nakatsuji, H.; Caricato, M.; Li, X.; Hratchian, H. P.; Izmaylov, A. F.; Bloino, J.; Zheng, G.; Sonnenberg, J. L.; Hada, M.; Ehara, M.; Toyota, K.; Fukuda, R.; Hasegawa, J.; Ishida, M.; Nakajima, T.; Honda, Y.; Kitao, O.; Nakai, H.; Vreven, T.; Montgomery, J. A., Jr.; Peralta, J. E.; Ogliaro, F.; Bearpark, M.; Heyd, J. J.; Brothers, E.; Kudin, K. N.; Staroverov, V. N.; Kobayashi, R.; Normand, J.; Raghavachari, K.; Rendell, A.; Burant, J. C.; Iyengar, S. S.; Tomasi, J.; Cossi, M.; Rega, N.; Millam, N. J.; Klene, M.; Knox, J. E.; Cross, J. B.; Bakken, V.; Adamo, C.; Jaramillo, J.; Gomperts, R.; Stratmann, R. E.; Yazyev, O.; Austin, A. J.; Cammi, R.; Pomelli, C.; Ochterski, J. W.; Martin, R. L.; Morokuma, K.; Zakrzewski, V. G.; Voth, G. A.; Salvador, P.; Dannenberg, J. J.; Dapprich, S.; Daniels, A. D.; Farkas, Ö.; Foresman, J. B.; Ortiz, J. V.; Cioslowski, J.; Fox, D. J. *Gaussian 09*, Revisions A.02 and D.01; Gaussian, Inc.: Wallingford, CT, 2009.

(32) Hohenberg, P.; Kohn, W. Inhomogeneous Electron Gas. *Phys. Rev.* **1964**, *136*, B864–B871.

(33) Møller, C.; Plesset, M. S. Note on the Approximation Treatment for Many-Electron Systems. *Phys. Rev.* **1934**, *46*, 618–622.

(34) Becke, A. D. Density-Functional Thermochemistry. III. The Role of Exact Exchange. *J. Chem. Phys.* **1993**, *98*, 5648–52.

(35) Lee, C.; Yang, W.; Parr, R. G. Development of the Colle-Salvetti Correlation-Energy Formula into a Functional of the Electron Density. *Phys. Rev. B* **1988**, *37*, 785–789.

(36) Perdew, J. P.; Burke, K.; Ernzerhof, M. Generalized Gradient Approximation Made Simple. *Phys. Rev. Lett.* **1996**, *77*, 3865–3868.

- (37) Chai, J.-D.; Head-Gordon, M. Systematic Optimization of Long-Range Corrected Hybrid Density Functionals. *J. Chem. Phys.* **2008**, *128*, 084106.
- (38) Raghavachari, K.; Binkley, J. S.; Seeger, R.; Pople, J. A. Self-Consistent Molecular Orbital Methods. 20. Basis Set for Correlated Wave-Functions. *J. Chem. Phys.* **1980**, *72*, 650–654.
- (39) Dunning, T. H., Jr. Gaussian Basis Sets for Use in Correlated Molecular Calculations. I. The Atoms Boron Through Neon and Hydrogen. *J. Chem. Phys.* **1989**, *90*, 1007–1023.
- (40) Grimme, S. Semiempirical GGA-type Density Functional Constructed with a Long-Range Dispersion Correction. *J. Comput. Chem.* **2006**, *27*, 1787–1799.
- (41) Koch, U.; Popelier, P. L. A. Characterization of C-H-O Hydrogen-Bonds on the Basis of the Charge-Density. *J. Phys. Chem.* **1995**, *99*, 9747–9754.
- (42) Bader, R. F. W. *AIMPAC, Suite of Programs for the Theory of Atoms in Molecules*; McMaster University: Hamilton, Ontario, Canada, 1991.
- (43) Schlegel, H. B. Estimating the Hessian for Gradient-Type Geometry Optimizations. *Theor. Chim. Acta* **1984**, *66*, 333–340.
- (44) Trouiller, N.; Martins, J. S. Efficient Pseudopotentials for Plane-Wave Calculations. *Phys. Rev. B* **1991**, *43*, 8861–8869.
- (45) Kittel, C. *Introduction to Solid State Physics*, 7th ed; Wiley: New York, 1996.
- (46) Monkhorst, H. J.; Pack, J. D. On Special Points for Brillouin Zone Integrations. *Phys. Rev. B* **1976**, *13*, 5188–5192.
- (47) Nosé, S. A Molecular Dynamics Method for Simulations in the Canonical Ensemble. *Mol. Phys.* **1984**, *52*, 255–268.
- (48) Nosé, S. A Unified Formulation of the Constant Temperature Molecular Dynamics Methods. *J. Chem. Phys.* **1984**, *81*, 511–519.
- (49) Hoover, W. G. Canonical dynamics: Equilibrium phase-space distributions. *Phys. Rev. A* **1985**, *31*, 1695–1697.
- (50) Hockney, R. W. The Potential Calculation and Some Applications. *Methods Comput. Phys.* **1970**, *9*, 136–211.
- (51) CPMD; Copyright IBM Corp., Zurich, Switzerland, 1990–2004; Copyright MPI fuer Festkoerperforschung Stuttgart, Stuttgart, Germany, 1997–2001.
- (52) Humphrey, W.; Dalke, A.; Schulten, K. VMD - Visual Molecular Dynamics. *J. Mol. Graphics* **1996**, *14*, 33–38.
- (53) Gnuplot; Williams, T.; Kelley, C. Copyright 1986–1993, 1998, 2004. Broeker, H. B.; Campbell, J.; Cunningham, R.; Denholm, D.; Elber, G.; Fearick, R.; Grammes, C.; Hart, L. et al.. Copyright 2004–2007.
- (54) Ozeryanskii, V. A.; Milov, A. A.; Minkin, V. I.; Pozharskii, A. F. 1,8-Bis(dimethylamino)naphthalene-2,7-diolate: A Simple Arylamine Nitrogen Base with Hydride-Ion-Comparable Proton Affinity. *Angew. Chem., Int. Ed.* **2006**, *45*, 1453–1456.
- (55) Marx, D. Proton Transfer 200 Years after von Grotthuss: Insights from Ab Initio Simulations. *ChemPhysChem* **2006**, *7*, 1848–1870.
- (56) Hassanali, A.; Giberti, F.; Cuny, J.; Kühne, T. D.; Parrinello, M. Proton Transfer Through the Water Gossamer. *Proc. Natl. Acad. Sci. U. S. A.* **2013**, *110*, 13723–13728.
- (57) Ceriotti, M.; Cuny, J.; Parrinello, M.; Manolopoulos, D. E. Nuclear Quantum Effects and Hydrogen Bond Fluctuations in Water. *Proc. Natl. Acad. Sci. U. S. A.* **2013**, *110*, 15591–15596.
- (58) Nachimuthu, S.; Gao, J.; Truhlar, D. G. A benchmark test suite for proton transfer energies and its use to test electronic structure model chemistries. *Chem. Phys.* **2012**, *400*, 8–12.
- (59) Jezierska-Mazzarello, A.; Panek, J. J.; Szatyłowicz, H.; Krygowski, T. M. Hydrogen Bonding as a Modulator of Aromaticity and Electronic Structure of Selected ortho-Hydroxybenzaldehyde Derivatives. *J. Phys. Chem. A* **2012**, *116*, 460–475.
- (60) Gaigeot, M.-P.; Sprik, M. Ab Initio Molecular Dynamics Computation of the Infrared Spectrum of Aqueous Uracil. *J. Phys. Chem. B* **2003**, *107*, 10344–10358.
- (61) Schwegler, E.; Grossman, J. C.; Gygi, F.; Galli, G. Towards an Assessment of the Accuracy of Density Functional Theory for First Principles Simulations of Water. II. *J. Chem. Phys.* **2004**, *121*, 5400–5409.
- (62) Tangney, P.; Scandolo, S. How Well Do Car–Parrinello Simulations Reproduce the Born–Oppenheimer Surface? Theory and Examples. *J. Chem. Phys.* **2002**, *116*, 14–24.
- (63) Wathelot, V.; Champagne, B.; Mosley, D. H.; André, J.-M.; Massidda, S. Vibrational Frequencies of Diatomic Molecules from Car and Parrinello Molecular Dynamics. *Chem. Phys. Lett.* **1997**, *275*, 506–512.
- (64) Steiner, T.; Majerz, I.; Wilson, C. C. First O–H–N Hydrogen Bond with a Centered Proton Obtained by Thermally Induced Proton Migration. *Angew. Chem., Int. Ed.* **2001**, *40*, 2651–2654.
- (65) Laio, A.; Parrinello, M. Escaping Free-Energy Minima. *Proc. Natl. Acad. Sci. U. S. A.* **2002**, *99*, 12562–12566.
- (66) Denisov, G. S.; Mavri, J.; Sobczyk, L. In *Hydrogen Bonding—New Insights (Challenges and Advances in Computational Chemistry and Physics)*, 3; Grabowski, S. J., Ed.; Springer: Dordrecht, 2006; pp 377–416.
- (67) Stare, J.; Eckert, J.; Panek, J.; Grdadolnik, J.; Mavri, J.; Hadži, D. Proton Dynamics in the Strong Chelate Hydrogen Bond of Crystalline Picolinic Acid N-oxide. A New Computational Approach and Infrared, Raman and INS Study. *J. Phys. Chem. A* **2008**, *112*, 1576–1586.